Journal of Fluids and Structures 17 (2003) 479–483

JOURNAL OF FLUIDS AND STRUCTURES

www.elsevier.nl/locate/jnlabr/yjfls

Brief Communication

A note on the fluid damping of an elastic cylinder in a cross-flow

H.J. Zhang[a], Y. Zhou[a,*], R.M.C. So[a], M.P. Mignolet[b], Z.J. Wang[a]

[a] *Department of Mechanical Engineering, The Hong Kong Polytechnic University, Hung Hom, Kowloon, Hong Kong*
[b] *Department of Mechanical and Aerospace Engineering, Arizona State University, Tempe, AZ 85287, USA*

Received 8 March 2000; accepted 17 May 2002

Abstract

This note reports an experimental study of the fluid damping of a long slender cylinder, fixed at both ends (no rotation and displacement), in a cross air-flow. The structural dynamic strain was measured in the lift direction over a range of reduced velocity U_r using a fibre-optic Bragg grating sensor. An auto-regressive moving average technique was used to deduce the effective damping ratios (including structural and fluid damping) from the strain data. The modal damping ratios corresponding to the first-, second- and third-mode vibrations over a range of U_r from 3 to 45 have been characterized and discussed. The results show that the value of fluid damping varied significantly at resonance when the vortex-shedding frequency coincides with one of the natural frequencies of the combined fluid–structure system.

1. Introduction

Damping models the energy dissipation of a system during vibration and plays an important role in the stability of a structure and its vibration amplitude. Its knowledge is essential if the dynamic behaviour of a structure in a cross-flow were to be understood thoroughly. Damping may arise from fluid surrounding the structure as well as from the structure. While structural damping is related to the properties of the structure, fluid damping originates from skin friction and fluid drag, i.e., the result of viscous shearing of the fluid at the surface of the structure and flow separation. As a result, fluid damping is motion dependent and is difficult to estimate (Weaver and Fitzpatrick, 1988; Granger et al., 1993).

Using an auto-regressive moving average (ARMA) technique, Zhou et al. (2000) and So et al. (2001) deduced the fluid damping ratios from the structural displacement time series obtained from a numerical simulation of an elastic cylinder in a cross-flow. The damping ratios thus deduced showed a trend quite similar to the experimental measurements of Griffin and Koopmann (1977). In comparison with the simulation data, signals obtained from experiments are usually 'noisier'. Thus, whether the ARMA technique is equally applicable for the analysis of experimental data remains to be verified. Furthermore, the mass ratio considered in the study of Zhou et al. (2000) is relatively small. For the case of a cylinder in air-flow, the mass ratio is much larger. How would this difference in mass ratio affect the fluid damping? The present work aims to study experimentally the effective damping ratio, including structural damping and fluid damping, of a long slender cylinder in a cross air-flow. The effective damping ratios of the first three modes were deduced from the measured signals using the ARMA technique. The results are discussed in detail, including the variation of the damping ratio over a relatively large range of reduced velocity U_r and its behaviour at resonance and off-resonance.

*Corresponding author. Tel.: +852-2766-6662; fax: +852-2365-4703.
E-mail address: mmyzhou@polyu.edu.hk (Y. Zhou).

0889-9746/03/$ - see front matter
PII: S0889-9746(02)00137-8

Nomenclature

d	diameter of circular cylinder (mm)
E_α	spectra of fluctuations α
f	frequency in spectrum analysis (Hz)
f_s	average vortex shedding frequency (Hz)
f_n'	the first-mode natural frequency of the structure measured in the still air (Hz)
f_{n_1}	measured first-mode natural frequency of the fluid–structure system (Hz)
f_{n_2}	measured second-mode natural frequency of the fluid–structure system (Hz)
f_n'''	measured third-mode natural frequency of the fluid–structure system (Hz)
$\mathscr{R}e$	Reynolds number$\equiv U_\infty d/v$
U_∞	free stream velocty (m/s)
U_r	reduced velocity$\equiv U_\infty f_n' d$
x, y, z	coordinates in streamwise, transverse and spanwise directions, respectively
Y	cross-flow bending displacement measured at mid-span of the cylinder by laser vibrometer (μm)
$Y_{\text{r.m.s.}}$	root mean square value of Y (μm)
ε	dynamic strains measured by fibre Bragg grating (FBG) sensors ($\mu\varepsilon$)
$\varepsilon_{\text{r.m.s.}}$	root mean square values of $\varepsilon(\mu\varepsilon)$
ζ	damping ratio
ζ_s	measured structural damping ratio
$\zeta_e, \zeta_e'', \zeta_e'''$	effective first-, second- and third-mode damping ratios
ζ_f	fluid damping ratio
v	fluid kinematic viscosity

The ARMA modelling technique is based on the observation that the sampled response of a multi-degree-of-freedom system satisfies a linear recurrence relation (Mignolet and Red-Horse, 1994; Jadic et al., 1998). Consequently, ARMA modelling is not limited to single-mode behaviour; it identifies all modal characteristics present in the responses including possible outside dynamics, such as turbulence in the incoming flow. Furthermore, the estimation of the ARMA parameters accounts for the presence of modelling noise so that its effect on the computed damping ratios is significantly reduced. Finally, ARMA models have been shown (Jadic et al., 1998) to capture some nonlinear effects through the modelling of the higher harmonics content present in the response. These advantages of ARMA modelling far outweigh the increase in computational effort required to obtain reliable estimates of the damping ratios.

Granger (1990) developed a digital signal processing method for modal analysis of fluid–structure systems. This method is a multi-degree-of-freedom time domain method based on a development in the field of time-series analysis. The method was used to deduce fluid damping from the strain data of a cylinder placed in a square in-line tube bundle (Granger et al., 1993). Since their test cylinder, which was mounted on flexible support, was rigid, their system is different from that of a flexible cylinder on fixed supports as considered in this note. The formulation of Granger (1990) is in fact a specific ARMA model. However, there are some differences between his and the present formulation. For example, Granger (1990) used the same operator for auto-regressive (AR) and moving average (MA), as evident in Eq. (4), while the present technique has unequal operators for AR and MA and seeks the nonlinear maximum-likelihood solution. Granger further computed the ARMA coefficients A_k, B_k and C_k (in Eq. (2)) based on the auto-correlation of the measured signal, i.e., the ARMA model is applied on the correlation and then the noise term w is truly a noise. On the other hand, the present approach works directly with the measured signal. One benefit of this approach is that w denotes any measurement noise plus a fictitious random source that creates the randomness in the response and can physically be associated with the origin of the turbulence in the signal.

In this work, the experiment was carried out in a wind tunnel using a cylinder with a small diameter ($d \approx 6$ mm) over U_r range of 3–45 ($\mathscr{R}e = 800 - 11\,000$). Thus, the mass ratio, i.e., the cylinder mass over the virtual mass of the fluid, is large compared to that of a liquid–structure system. Within this velocity and mass ratio range and due to the smallness of d, the amplitude of vibration is expected to be very small. A Polytec Series 3000 Dual Laser Beam Vibrometer was used to measure the transverse bending displacement Y at the mid-span of the cylinder. The root mean square (r.m.s.) displacement, $Y_{\text{r.m.s.}}/d$, was estimated to be about 0.01. An optical FBG sensor was developed to measure the strain, ε, in a vibrating cylinder fixed at both ends (Zhou et al., 1999; Jin et al., 2000). The FBG sensor was located at mid-span of the cylinder. Since the sensor grating has a finite length of about 10 mm, the measurement represents the average strain over this length. The measured strain due to lift was consistent with the transverse displacement obtained using a laser

vibrometer; an empirical correlation between them was established in Zhou et al. (1999), where measurements were conducted under the same experimental conditions. When $U_r < 27$, the relation between $\varepsilon_{Y,\mathrm{r.m.s.}}$ and $Y_{\mathrm{r.m.s.}}$ is approximately linear. As the third-mode resonance, where the frequency of vortex shedding, f_s, coincides with the third-mode natural frequency of the fluid–cylinder system, occurs near $U_r \approx 27$, $\varepsilon_{Y,\mathrm{r.m.s.}}$ increases faster and the $\varepsilon_{Y,\mathrm{r.m.s.}} - Y_{\mathrm{r.m.s.}}$ relation starts to deviate from linearity. This deviation is not surprising. At a higher mode of vibration, Y experiences a faster spanwise variation for given amplitude. Consequently, ε, a second derivative of Y with respect to the spanwise variation, will increase faster than the displacement. The empirical correlation between $\varepsilon_{Y,\mathrm{r.m.s.}}$ and $Y_{\mathrm{r.m.s.}}$ implies that the measured strain may provide identical information on displacement for $U_r < 27$. Caution has to be taken to deduce information on displacement from the strain data at the occurrence of the third-mode resonance. One good point about the FBG measured strain is its reliability, reproducibility and the ease with which the technique works. It is also virtually nonintrusive much like the laser vibrometer technique. In view of this, the various parameters of fluid–cylinder interaction could be deduced with confidence. The present study is justified on this basis, namely, to make use of the FBG sensor to examine the physics of damping in a fix-supported cylinder vibrating in a cross-flow. This is why the study can be carried out in spite of the small vibration amplitudes of the cylinder.

In still air, the damping ratio (includes material damping and frictional losses at the supports as well as still air damping) has been determined from a plucking test and the result is $\zeta_s' \approx 0.032$. The first-mode natural frequency in still air has also been measured and has a value of 94 Hz. Thus, the second- and third-mode natural frequencies may be estimated to be 259 and 508 Hz, respectively (e.g., Zhou et al., 2001).

2. Results and discussion

The dependence of r.m.s. strain, $\varepsilon_{\mathrm{r.m.s.}}$, on U_r is shown in Fig. 1. Peaks in $\varepsilon_{\mathrm{r.m.s.}}$ are discernible at $U_r \approx 5$, 11 and 27. They can be identified from the spectral analysis with resonance occurring when the vortex shedding frequency is equal to the first-, second- and third-mode natural frequencies, f_n', f_n'' and f_n''', respectively. The peaks at $U_r \approx 5$ and 11 are very weak, probably because the flow excitation energy at these U_r are relatively small. The peak at $U_r \approx 27$ is most prominent.

The dominant vibration modes can be identified from the spectral analysis of the signals, as calculated using the ARMA technique. Fig. 2 presents the power spectra E_ε of ε at $U_r = 27$ where the third-mode resonance occurs. The peak at $f^* = fd/U_\infty = 0.016$ (an asterisk denotes normalization by U_∞ and d) in Fig. 2 has been experimentally verified to be the same as a wind tunnel natural vibration frequency. It is evident that the first three cylinder vibration modes play an important role. The following discussion will focus on the three modes of cylinder vibration and their relation with each other for the U_r range investigated.

The effective damping ratios, ζ_e', ζ_e'' and ζ_e''', are presented in Fig. 3. The number of points used for the ARMA estimation could have a significant impact on the result. In the present calculation, 120 000 data points were used, which was found to be sufficient to produce converged damping ratios. In the use of the ARMA technique, a model of a higher order provides in general a better fit to the original time series. However, a higher-order model demands more computing time. In the process of analysing numerical simulation data, Zhou et al. (2000) found that an order of 70 was

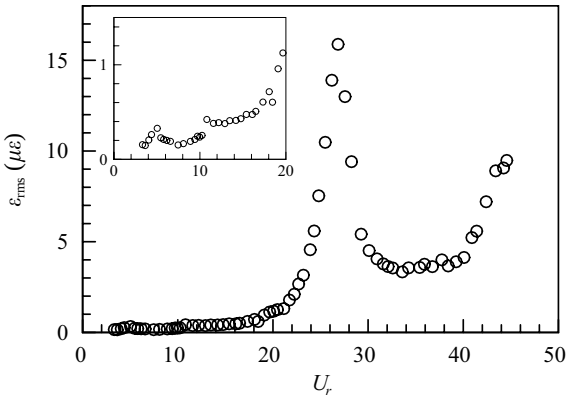

Fig. 1. Variation of $\varepsilon_{\mathrm{r.m.s.}}$ with U_r.

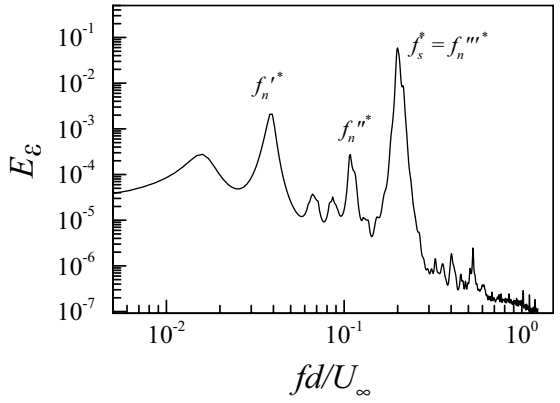

Fig. 2. Power spectra E_ε of ε, ($\mathscr{R}e = 6400$ or $U_r = 27$).

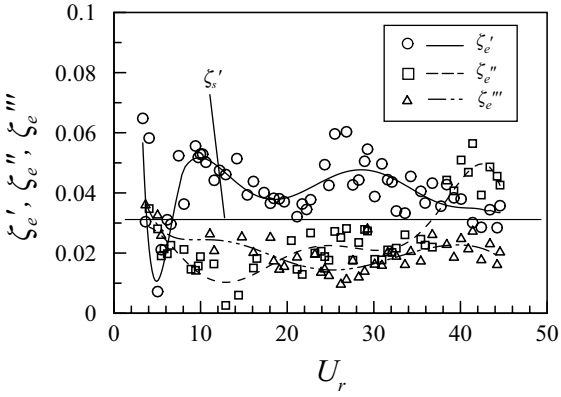

Fig. 3. Effective damping ratios: ζ_e' (first mode), ζ_e'' (second mode) and ζ_e''' (third mode). The horizontal solid line denotes the structural damping ratio ζ_s' measured in the still air.

sufficient. Experimental data is 'noisier' than numerical simulation data. In the present investigation, consistent results were achieved when an order of 190 was chosen. Note that the large value of the AR order is partly necessitated by the nonlinearity of the fluid–structure system, which implies the presence in the response of a large number of harmonics of the shedding frequency. These frequencies are genuine characteristics of the response and are automatically included in the ARMA model. The data exhibit scattering, as one would expect. Curves in Fig. 3, obtained by applying a seventh-order polynomial fit to the data points for different U_r ranges, indicate the trend only. The value of ζ_e' fluctuates about 0.04, larger than ζ_s', except near resonance.

At $U_r \approx 5$, where the first-mode resonance occurs, the first-mode effective damping ratio ζ_e' drops below the structural damping ζ_s' and approaches zero, implying a negative fluid damping ratio ζ_f'. The second- and third-mode damping ratios, ζ_e'' and ζ_e''', display a trough at $U_r \approx 11$ and 27 where f_s synchronizes with f_n'' and f_n''', respectively. Interestingly, ζ_e'' approaches a peak value around $U_r \approx 11$ and 27, while ζ_e''' continues to rise at $U_r \approx 5$. It seems that when one effective modal damping ratio dives because of synchronization, the others tend to rise. In general, the effective modal damping in the second and third modes is less than that of the first mode, viz. ζ_e''', $\zeta_e'' < \zeta_e'$. The present result is consistent with Blevins' (1975) observation that the structural damping corresponding to the third-mode vibration was lower than that of the first mode, even for this case of small fluid damping. This result could partially account for the relatively large vibration observed at $U_r \approx 27$.

For a quasi-steady vibration, the energy loss from a structure should be balanced by the energy imparted to the structure by the surrounding moving fluid. At the third-mode resonance, the vibration amplitude is relatively large, as inferred from $\varepsilon_{\text{r.m.s.}}$ (Fig. 1). The effective modal damping ratio corresponding to the third-mode resonance displays its minimum, 0.01. On the other hand, at this value of U_r (27) the ratios corresponding to the first and second modes show peaks at about 0.06 and 0.028, respectively. Evidently at $U_r = 27$, the flow transfers most of its energy to the cylinder

through the third-mode motion. However, Fig. 2 shows that significant motions are also induced in the first and second modes, which are not in phase with the dominant third-mode motion. Note that, since $\varepsilon_{\text{r.m.s.}}$ is approximately linearly correlated with $Y_{\text{r.m.s.}}$ for $U_r < 27$ but increases faster than Y at the occurrence of the third-mode resonance, the difference between the first- (or second-) and third-mode displacements may not be so great as the $\varepsilon_{\text{r.m.s.}}$ variation (Fig. 1) suggests. As the effective modal damping in flowing fluid is likely to be vibration amplitude dependent, this could account for the local maxima in the effective damping of the first and second modes during the third-mode resonance. Similar arguments are also applicable for resonance occurring at other modes.

Acknowledgements

Y.Z. and R.M.C.S. wishes to acknowledge support given to them by the Central Research Grant of The Hong Kong Polytechnic University under Grant No. G-V529, and the Research Grants Council of the Government of the Hong Kong Special Administrative Region under Grant Nos. PolyU5161/97E and PolyU5128/98E. Authors would also like to give special thanks to Prof. D.S. Weaver for his valuable comments and detailed suggestions.

References

Blevins, R.D., 1975. Vibration of a loosely held tube. ASME Journal of Engineering for Industry 97, 1301–1304.

Granger, S., 1990. A new signal processing method for investigating fluid elastic phenomena. Journal of Fluids and Structures 4, 73–97.

Granger, S., Campistron, R., Lebret, J., 1993. Motion-dependent excitation mechanisms in a square in-line tube bundle subject to water cross-flow: an experimental modal analysis. Journal of Fluids and Structures 7, 521–550.

Griffin, O.M., Koopmann, G.H., 1977. The vortex-excited lift and reaction forces on resonantly vibrating cylinders. Journal of Sound and Vibration 54 (3), 435–448.

Jadic, I., So, R.M.C., Mignolet, M.P., 1998. Analysis of fluid–structure interactions using a time-marching technique. Journal of Fluids and Structures 12, 631–654.

Jin, W., Zhou, Y., Chan, P.K.C., Xu, H.G., 2000. An optical fibre Bragg grating sensor for flow-induced structural vibration measurement. Sensors and Actuators 79, 36–45.

Mignolet, M.P., Red-Horse, J.R., 1994. ARMAX identification of vibrating structures: model and model order estimation. Proceedings of the 35th Structures, Structural Dynamics, and Materials Conference, AIAA/ASME, Hilton Head, South Carolina, 18–20 April , pp. 1628–1637.

So, R.M.C., Liu, Y., Chan, S.T., Lam, K., 2001. Numerical studies of a freely vibrating cylinder in a cross flow. Journal of Fluids and Structures 15, 845–866.

Weaver, D.S., Fitzpatrick, J.A., 1988. A review of cross-flow induced vibrations in heat exchanger tube arrays. Journal of Fluids and Structures 2, 73–93.

Zhou, Y., So, R.M.C., Jin, W., Xu, H.G., Chan, P.K.C., 1999. Dynamic strain measurements of a circular cylinder in a cross flow using a fibre Bragg grating sensor. Experiments in Fluids 27, 359–367.

Zhou, C.Y., So, R.M.C., Mignolet, M.P., 2000. Fluid damping of an elastic cylinder in a cross flow. Journal of Fluids and Structures 14, 303–322.

Zhou, Y., Wang, Z.J., So, R.M.C., Xu, S.J., Jin, W., 2001. Free vibrations of two side-by-side cylinders in a cross flow. Journal of Fluid Mechanics 443, 197–229.